Rock and Soil Mechanics

Volume 41 | Issue 12 Article 9

4-29-2021

Treatment of two boundary conditions for rainfall infiltration in slope and its application

Geng-qian NIAN

Zhong-hui CHEN

Ling-fan ZHANG

Min BAO

See next page for additional authors

Custom Citation

NIAN Geng-qian, CHEN Zhong-hui, ZHANG Ling-fan, BAO Min, ZHOU Zi-han . Treatment of two boundary conditions for rainfall infiltration in slope and its application[J]. Rock and Soil Mechanics, 2020, 41(12): 4105-4115.

Treatment of two boundary conditions for rainfall infiltration in slope and its application

Authors

Geng-qian NIAN, Zhong-hui CHEN, Ling-fan ZHANG, Min BAO, and Zi-han ZHOU

Rock and Soil Mechanics 2020 41(12): 4105−4115 ISSN 1000−7598
https: //doi.org/10.16285/j.rsm.2020.5338 rocksoilmech.researchcommons.org/journal

Treatment of two boundary conditions for rainfall infiltration in slope and its application

NIAN Geng-qian, CHEN Zhong-hui, ZHANG Ling-fan, BAO Min, ZHOU Zi-han
School of Mechanics and Civil Engineering, China University of Mining and Technology, Beijing 100083, China

Abstract: Using the Richards' equation of saturated-unsaturated seepage, the commercial Multiphysics finite element software COMSOL is adopted to deduce the governing equations of two boundary conditions with the pore water pressure as the control variable for the infiltration and seepage (overflow) boundary conditions in the rainfall infiltration problem of slope. Based on the two-dimensional soil column model and the published models, the value of the boundary coupling length scale L in the governing equation is discussed, and L equal to 0.001 m is found reasonable. A simple two-dimensional slope model is then established, and the governing equations of the above boundary conditions are applied to analyze the infiltration and seepage law of rainfall with different intensities (long and weak, short and strong). The results show that when the rainfall intensity is 4 mm /h, the actual infiltration rate is always equal to the rainfall intensity, and the water content of the surface soil has increased from 0.29 to 0.35. When rainfall lasts for 75 h, the surface seepage occurs at the foot of the slope, the total infiltration amount of the study area at 200 h is 39.068 m^3; when the rainfall intensity is 40 mm /h, the actual infiltration rate first equals the rainfall intensity, and then gradually decreases, and the water content of the surface soil increases from 0.29 to 0.415 (saturated). When rainfall lasts for 4 h, the surface seepage occurs at the foot of the slope, the total infiltration of study area at 20 h is 26.908 m^3, which is far less than the former. This conclusion is consistent with the existing rainfall infiltration law in slope, which further proves the reliability of the above boundary condition governing equations that provides a feasible method for the boundary condition problem in finite element analysis of rainfall in slope.

Keywords: slope; rainfall infiltration; Richards' equation; boundary condition; governing equation

1 Introduction

The problem of slope rainfall infiltration involves two boundary conditions, namely, infiltration boundary conditions and seepage (overflow) boundary conditions. Under complex rainfall conditions, the seepage process of both boundary conditions is a continuous conversion process between the flow boundary (Neumann boundary) and the pressure boundary (Dirichlet boundary). Therefore, the processing of boundary conditions has always been a key issue in numerical calculation. There have been many studies on the treatment of boundary conditions. Wu et al.[1] directly set the infiltration velocity, namely rainfall intensity, on the slope surface to analyse the transient seepage field caused by rainfall infiltration. Li et al.[2] took the saturation permeability coefficient as the control condition and used Fortran language to develop an iterative code to calculate the transient permeability coefficient of each node. If the saturation permeability coefficient is greater than the pressure coefficient, it is the pressure boundary; otherwise, it is the flow boundary. Zhang et al.[3] took the infiltration rate as the control condition and calculated the infiltration rate of the boundary through an iterative procedure according to the finite element Galerkin method. If the rainfall intensity was greater than the infiltration rate, it was the pressure boundary and vice versa. Rong et al.[4] wrote the unsaturated seepage flow program SUSC, which took the maximum infiltration capacity as the control condition, calculated through the maximum infiltration capacity equation in the iterative calculation process, and constantly compared with the given potential surface flux. If less than the latter, the boundary flux is the maximum infiltration capacity, and vice versa is the fixed surface flux. In FLAC3D, Jiang et al.[5] conducted secondary development through FISH language and took saturation permeability coefficient as the control condition. If rainfall intensity is greater than saturation permeability coefficient, boundary flux is rainfall intensity and vice versa. Jiang et al.[6] compared the infiltration rate with the rainfall intensity and obtained the time t_p of infiltration rate equal to the rainfall intensity. When the rainfall time was less than t_p, it was the flow boundary; otherwise, it was the pressure boundary. Wang et al.[7] applied a thin layer of air unit on the soil surface to describe the dynamic boundary conditions and realized the infiltration under the runoff condition.

The treatment methods of the above boundary conditions all have certain limitations. First of all, the conversion

Received: 25 March 2020 Revised: 16 June 2020
This work was supported by the National Key Research and Development Program of China (2016YFC0801602, 2017YFC1503103).
First author: NIAN Geng-qian, male, born in1994, Master degree candidate, majoring in slope engineering. E-mail: nian_gq@163.com

of boundary conditions from flow boundary to pressure boundary condition is ignored when the infiltration velocity is directly given, and the error is relatively large. Second, the saturated permeability coefficient and the infiltration rate are not the same as the largest water infiltration capacity (pressure boundary conditions of the actual infiltration rate controlled by the largest water infiltration capacity), and the largest water infiltration capacity is a nonlinear change of amount, very complicated to calculate. The quantity cannot be determined before the pressure field being obtained and can only be assumed in advance and gradual adjustment. Finally, the flow of rainwater is related to the specific parameters of the air unit, which is difficult to determine. In addition, practical examples where seepage boundary conditions are considered in the analysis of slope rainfall infiltration are even rarer. Therefore, this article using the commercial finite element code COMSOL-Multiphysics, with the pore water pressure as the conditions (to avoid the problem of the maximum infiltration ability difficult to be determined), the infiltration boundary condition is deduced and the control equation of seepage boundary conditions is verified with examples in the existing literature. Finally, the two boundary conditions are applied to the two-dimensional slope model to analyse the seepage law on the surface and inside of the slope under two different rainfall conditions (strong and weak, short and long). As a result, this study provides a novel method of support for the finite element analysis of slope rainfall infiltration.

2 Saturated−unsaturated seepage differential equation

Darcy's Law is used to describe the equation of fluid flow in porous media, but it is mostly used to solve the saturated seepage flow of rock and soil mass. If the pore water pressure is taken as an independent variable, its differential form is expressed as follows[8]:

$$\boldsymbol{u} = -\frac{K_s}{\rho g}\left(\nabla p + \rho g \nabla D\right) \tag{1}$$

where $\boldsymbol{u}$ is the velocity of boundary; K_s is saturation permeability coefficient; p is pore water pressure; ρ is fluid density; g is the acceleration of gravity; and D is the vertical coordinate (positive upward).

Without considering the source terms such as evaporation and water exchange, the continuity differential equation of the fluid is written as follows[9−10]:

$$\frac{\partial(\rho\varepsilon)}{\partial t} + \nabla\cdot(\rho\boldsymbol{u}) = 0 \tag{2}$$

where ε is the porosity.

By substituting Eq. (1) into Eq. (2), the saturated seepage differential equation can be obtained as follows:

$$\frac{\partial(\rho\varepsilon)}{\partial t} + \nabla\cdot\rho\left[-\frac{K_s}{\rho g}\left(\nabla p + \rho g\nabla D\right)\right] = 0 \tag{3}$$

Let's expand out $\frac{\partial(\rho\varepsilon)}{\partial t}$ and get:

$$\frac{\partial(\rho\varepsilon)}{\partial t} = \varepsilon\frac{\partial\rho}{\partial t} + \rho\frac{\partial\varepsilon}{\partial t} \tag{4}$$

Then, the porosity and the fluid density are defined as functions of pore water pressure, and the following equation can be obtained:

$$\frac{\partial(\rho\varepsilon)}{\partial t} = \varepsilon\frac{\partial\rho}{\partial p}\frac{\partial p}{\partial t} + \rho\frac{\partial\varepsilon}{\partial p}\frac{\partial p}{\partial t} \tag{5}$$

The compressibility of the fluid can be expressed as follows[11]:

$$x_f = \frac{1}{\rho}\cdot\frac{\partial\rho}{\partial p} \tag{6}$$

The effective compressibility of the matrix can be expressed as[12]:

$$x_p = \frac{\partial\varepsilon}{\partial p} \tag{7}$$

By substituting Eq. (6) and Eq. (7) into Eq. (5), it can be obtained:

$$\frac{\partial(\rho\varepsilon)}{\partial t} = \rho\left(\varepsilon x_f + x_p\right)\frac{\partial p}{\partial t} \tag{8}$$

In COMSOL, the water storage model S(1/Pa) can be expressed as[11]

$$S = \varepsilon x_f + x_p \tag{9}$$

Substituting into Eqs. (8) and (3) yields the partial differential form of saturated seepage of rock and soil mass as follows:

$$\rho S\frac{\partial p}{\partial t} + \nabla\cdot\rho\left(-\frac{K_s}{\rho g}\left(\nabla p + \rho g\nabla D\right)\right) = 0 \tag{10}$$

The Richards equation is the basic equation of unsaturated seepage theory, and is extended to the saturated−unsaturated seepage equation. The pressure head is taken as the independent variable. Its partial differential equation is as follows[13]:

$$\left(C + S_e S_s\right)\frac{\partial h_p}{\partial t} - \nabla\cdot\left[K\left(\nabla h_p + \nabla D\right)\right] = 0 \tag{11}$$

where C is the specific water capacity ($\mathrm{d}\theta/\mathrm{d}h$); S_s is the water storage rate (1 /m); θ is the volumetric water content; S_e is the effective saturation; h_p is the pressure head;

and K is the unsaturated permeability coefficient.

The water storage rate S_s can be expressed by[14]

$$S_s = \rho g\left(\varepsilon x_f + x_p\right) \tag{12}$$

The unsaturated permeability coefficient is a constantly changing quantity, and its calculation formula will be

$$K = K_s k_r \tag{13}$$

where k_r is the relative permeability coefficient.

Equation (11) is transformed into Richards equation expressed by pore water pressure p:

$$\rho\left(\frac{C}{\rho g} + S_e S\right)\frac{\partial p}{\partial t} - \nabla\cdot\rho\left[\frac{K_s k_r}{\rho g}\left(\nabla p + \rho g \nabla D\right)\right] = 0 \tag{14}$$

Equation (14) is a partial differential equation describing saturated−unsaturated seepage of rock and soil mass with pore water pressure p as an independent variable. When the rock and soil mass reaches saturation, the effective saturation S_e is 1, the specific water capacity C is 0, and the relative permeability coefficient k_r is 1, this equation becomes a saturated seepage differential equation, namely, Eq. (10). Unsaturated hydraulic parameters C, S_e, k_r, and θ can be calculated by Van Genuchten model[15] or Brooks-Corey model[16].

3 Treatment of two boundary conditions

3.1 Boundary conditions of infiltration

For the rainfall infiltration of the slope, when the rainfall intensity is less than the saturated permeability coefficient of the rock and soil mass of a slope, the surface soil saturation of the slope increases but will not reach saturation. The infiltration rate is always equal to the rainfall intensity, and the infiltration boundary condition is the flow boundary. It can be known from the conservation of mass law that:

$$-\boldsymbol{n}\cdot\rho\boldsymbol{u} = \rho R \tag{15}$$

where $\boldsymbol{n}$ is the outer normal vector of the boundary; and R is the rainfall intensity.

When the rainfall intensity is greater than the saturated permeability coefficient of the rock and soil mass of the slope, all the rainwater begins to penetrate into the rock and soil mass, and the infiltration boundary condition is the flow boundary. Then, the surface soil of the slope reaches saturation in a short time, forming a transient saturation zone. At this time, the rainwater is divided into two parts: one flows into the soil, the other part forms surface runoff and a certain amount of hydrops remain on the surface of the slope, and the infiltration boundary condition becomes a pressure boundary. For the flow boundary stage, its infiltration rate equals the rainfall intensity, hence Eq. (15) can be used to express it. When the infiltration boundary is at the pressure boundary stage, its permeability property is equivalent to a semi-permeable layer. The medium in the model domain is connected to a larger water body through the semi-permeable layer, here refers to the hydrops on the surface of the rock and soil. The flow rate of the external fluid source flowing into the model domain through the semi-pervious layer is related to the water head difference on both sides of the semi-pervious layer and the conductivity of the semi-pervious layer to the fluid, and it can be known from the mass conservation law that:

$$-\boldsymbol{n}\cdot\rho\boldsymbol{u} = \rho R_b\left(H_b - H\right) \tag{16}$$

where H_b is the head of the fluid source outside the semi-permeable layer; H is the water head of the model domain in the semi-permeable layer; and R_b is the conductivity of the semi-permeable layer to the fluid under the action of head difference.

In general, the conductivity R_b of the semi-permeable layer to the fluid can be obtained by the following formula[11]:

$$R_b = \frac{K_b}{B} \tag{17}$$

where K_b is the permeability coefficient of the medium in the semi-permeable layer; and B is the thickness of the semi-permeable layer.

If the infiltration boundary under the pressure boundary is regarded as a semi-permeable layer, the medium is the rock and soil mass of slope, the permeability coefficient can be taken as the saturated permeability coefficient K_s of the rock mass. Since the thickness of the infiltration boundary is an equivalent physical quantity that cannot be measured, the coupling length scale L can be used to replace it first. Then the conductivity of the infiltration boundary to water under pressure boundary conditions can be expressed by the following equation:

$$R_b = \frac{K_s}{L} \tag{18}$$

Rainfall infiltration in a two-dimensional soil column model is taken as an example. When hydrops forms on the soil surface, the infiltration state is shown in Fig. 1. The soil height is Z, the soil bottom is taken as the reference line of the water head at position 0, and the total water heads at the upper and lower infiltration boundaries are written respectively:

$$H_b = Z + H_w \tag{19}$$

$$H = Z + \frac{p}{\rho g} \tag{20}$$

where H_w is the hydrops depth; Z is the position head; and p is the pore water pressure on the surface under the infiltration boundary, which is obtained by iterative calculation of finite element code.

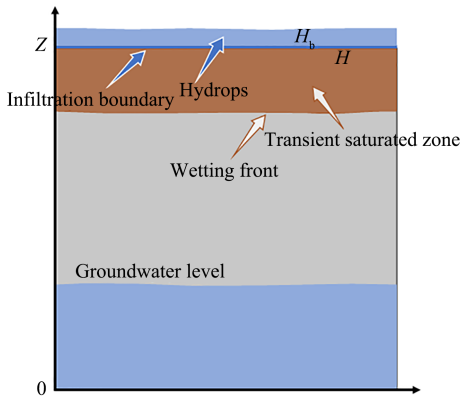

Fig. 1 Diagram of hydrops infiltration

Substituting Eqs. (18)−(20) into Eq. (16) results in

$$-\boldsymbol{n}\cdot\rho\boldsymbol{u} = \rho\frac{K_s}{L}\left(H_w - \frac{p}{\rho g}\right) \tag{21}$$

The pore water pressure p is used to control the transformation of infiltration boundary conditions. Expressing α as a function of p, its equation is written as follows:

$$\left.\begin{aligned}\alpha = 1 \quad p < 0\\ \alpha = 0 \quad p \geqslant 0\end{aligned}\right\} \tag{22}$$

In order to prevent numerical results from not converging due to numerical mutation, the function α should be set as a part of the smooth segment, as plotted in Fig. 2.

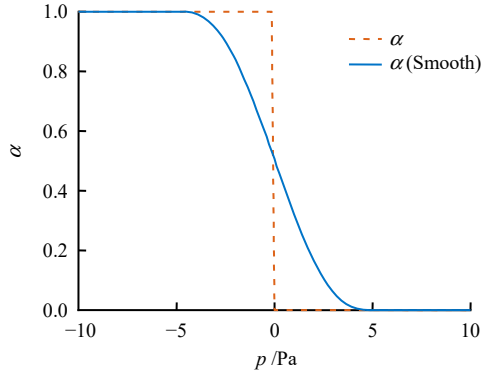

Fig. 2 Relationship between the function α and p

Let:

$$\beta = 1 - \alpha \tag{23}$$

where α and β together are called complementary smoothing functions.

Complementary smoothing function is used to combine the flow boundary equation and pressure boundary equation, thus, the governing equation of rainfall infiltration boundary condition is obtained as follows:

$$-\boldsymbol{n}\cdot\rho\boldsymbol{u} = \rho\left[\alpha R + \beta\frac{K_s}{L}\left(H_w - \frac{p}{\rho g}\right)\right] \tag{24}$$

When p is smaller than 0, α is equal to 1, β is equal to 0, and Eq. (24) is transformed into Eq. (15), representing the infiltration boundary of the flow boundary stage; when p is greater than or equal to 0, α is equal to 0, β is equal to 1, and Eq. (24) is transformed into Eq. (21), representing the infiltration boundary of the pressure boundary stage. From the governing equation, the conversion of infiltration boundary conditions can be controlled according to the calculation results of pore water pressure in the surface soil during the finite element calculation only by using the equation to represent the velocity of infiltration boundary and specifying relevant parameters such as rainfall intensity, saturated permeability coefficient, hydrops depth, etc.

In order to discuss the reasonable value of coupling length scale L (m), this study takes a two-dimensional soil column model with a length and height of 1 m as the research object, values L from large to small, and analyses the relationship between actual infiltration rate and L through numerical calculation. The upper boundary of the model is the rainfall infiltration boundary, the left and right boundaries are no-flow boundaries, and the lower boundary is a permeable layer boundary, as shown in Fig. 3. The unsaturated hydraulic parameters are calculated using the Van Genuchen model. The initial conditions are expressed as pressure head and the soil is sand. The relevant parameters are provided in Table 1.

Table 1 Relevant hydraulic parameters for calculation

Saturated volumetric water content θ_s	Residual volumetric water content θ_r	Saturated permeability coefficient K_s /(m • s^{-1})	Initial condition H_p /m	Van Genuchen constant			Rainfall intensity /(m • s^{-1})
				α	n	l	
0.4	0.04	1×10^{-6}	−0.4	2.5	2.1	0.5	$4K_s$

Different values of L (m) are used for finite element calculation. In order to reflect the conversion of infiltration boundary conditions, rainfall intensity is set as 4 times of saturated permeability coefficient. The variation rule of actual infiltration rate of infiltration boundary calculated with time is shown in Fig. 4. Since the Richards equation has a strong nonlinear characteristic, there will be a certain fitting process in the initial stage of calculation, and the

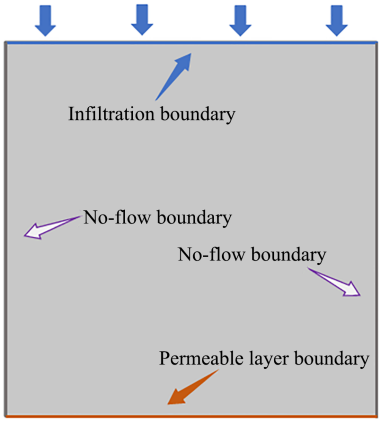

Fig. 3 Two-dimensional soil column model

calculation results during this period can be ignored. It can be seen from the figure that the calculated results reflect the change rule of the actual infiltration rate starting from 10 minutes. In the flow boundary condition, the actual infiltration rate of the boundary is equal to the rainfall intensity, independent of the magnitude of L. At 22 minutes, the surface soil reaches saturation, and the boundary condition is converted to the pressure boundary. As can be seen from the curve, when the magnitude of L is 10^0 and 10^2, the change law of the actual infiltration rate is the same, but the value is small. When the magnitude of L is 10^{-2} and 10^{-3}, the value of the actual infiltration rate increases. When the magnitude of L is 10^{-4}, the value of the actual infiltration rate is the same as that when L is 10^{-3} and does not increase.

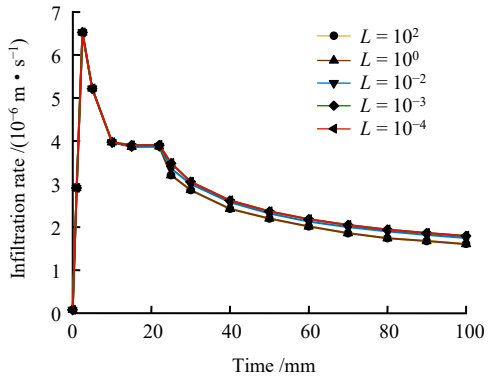

Fig. 4 Relationship between actual infiltration rate and *L*

Under the conditions of different values of L, the actual infiltration rate at some moments is shown in Table 2. By combining with Fig. 4 it is shown that under the stress boundary condition, when the magnitude of L value is less than 10^{-3}, the actual infiltration rate is relatively small; when the magnitude of L value is greater than 10^{-3}, the values of the actual infiltration rate is equal to that when the magnitude of L value is10^{-3}. Therefore, for the sake of convenience, L can have a unique value 10^{-3}.

Table 2 Actual infiltration rate at some moments under different *L* conditions

L	Infiltration rate at different times /(m • s^{-1})				
	10	22	30	60	100
10^2	3.970	3.874	2.859	2.016	1.603
10^0	3.970	3.874	2.859	2.016	1.603
10^{-2}	3.970	3.885	3.003	2.128	1.747
10^{-3}	3.970	3.914	3.053	2.181	1.794
10^{-4}	3.970	3.914	3.054	2.183	1.794

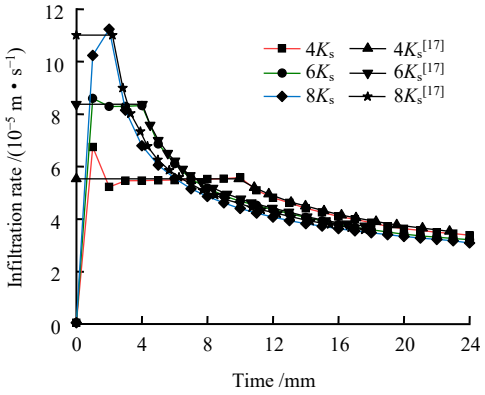

Fig. 5 Evolution curves of actual infiltration rate under different rainfall intensities

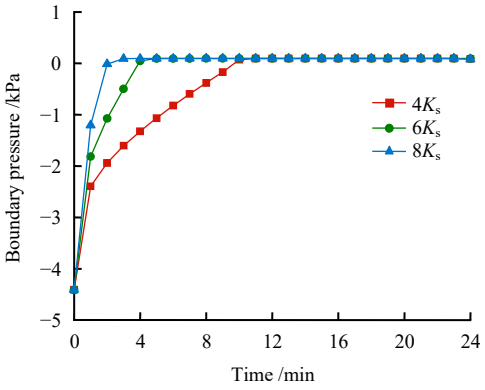

Fig. 6 Evolution curves of boundary pressure under different rainfall intensities

In order to verify whether the above equation describing the infiltration boundary conditions and the value of L (m) are reasonable, this study carries out finite element calculation for one of the infiltration models of Mein et al.[17]. The soil is sandy loam with a saturated permeability coefficient of 1.39×10^{-5} m /s and porosity of 0.518. May[18] fitted the Van Genuchten model with the soil water holding capacity and relative permeability curves provided by Mein et al.[17], obtained that the residual water content of the soil is 0.119 and the Van Genuchten parameters are 2.68 cm^{-1} and 4.36, respectively. The infiltration model is similar to the two-dimensional soil column model in

Fig. 3, only the height is increased to 2 m. Under the circumstance that the infiltration depth is less than 1 m, the two-dimensional soil column model can still be used in the numerical model without changing the boundary conditions. Initial conditions are expressed as pressure water head with a value of −0.45 m, and rainfall intensity is 4, 6, and 8 times of saturated permeability coefficient, respectively.

Figure 5 compares the results of finite element simulation with those of Mein et al.[17], ignoring the fitting process at the beginning of the calculation, it is found that the results are in good agreement. As can be seen from the curves of rainfall intensity of $4K_s$ and $6K_s$, the first 2 minutes is a process of finite element calculation fitting. However, when the rainfall intensity of $8K_s$ is high, soil reaches saturation at about 2.1 minutes, hence the error of actual infiltration rate at this stage is large, but it does not affect the subsequent calculation results. The boundary pressure change under different rainfall intensity curves is shown in Fig. 6. As the rainfall continues, the pore water pressure gradually increases, and this stage is the flow boundary condition stage. When the soil is saturated, the boundary pressure increases to a constant value, which is 95.76 Pa in the figure. This stage is the pressure boundary condition stage. The water depth set by this simulation is 0.01 m, and the calculation shows that the pressure of the surface soil at saturation is 100 Pa, which is close to the previous one.

3.2 Seepage boundary conditions

In slope rainfall infiltration analysis, seepage (overflow) boundary is very important and needs to be considered. When the rainfall infiltration causes the rise of groundwater level in the body, the slope or the slope body is partially saturated soils, water is seeping outward from the slope body. At present, however, the treatment of seepage boundary is neglected in most slope rainfall numerical calculation. For the seepage boundary, when the body of the slope is unsaturated, the water will not seep out. But when the body of the slope is saturated, the water will continue to seep out. Referring to the method of rainfall infiltration boundary, the seepage boundary can still be expressed by a similar equation, as follows:

$$-\boldsymbol{n}\cdot\rho\boldsymbol{u}=\rho\left[\alpha I+\beta R_{\mathrm{b}}\left(H_{\mathrm{b}}-H\right)\right] \tag{25}$$

where I is the flow velocity of the boundary under the unsaturated condition. For the seepage boundary, I is equal to zero. R_{b} is the conductivity of the semi-permeable layer to fluid; H_{b} is the water head outside the boundary; and H is the internal water head of the boundary.

When the soil in a certain area of the slope reaches saturation, the total water head inside and outside the seepage boundary is written respectively:

$$H_{\mathrm{b}}=Z \tag{26}$$

$$H=Z+\frac{p}{\rho g} \tag{27}$$

Substituting Eqs. (18), (26) and (27) into Eq. (25) and simplifying, we can obtain:

$$-\boldsymbol{n}\cdot\rho\boldsymbol{u}=\rho\left[\gamma\frac{K_{\mathrm{s}}}{L}\left(-\frac{p}{\rho g}\right)\right] \tag{28}$$

where γ is a smoothing function.

γ is expressed as a function of pore water pressure p, as follows:

$$\left.\begin{array}{ll}\gamma=0 & p<0\\ \gamma=1 & p\geqslant 0\end{array}\right\} \tag{29}$$

In order to prevent numerical results from not converging due to abrupt changes in values, the function γ should also be set as a part of the smooth segment, as shown in Fig. 7.

In order to explore the reasonable value of coupling length scale L (m), a two-dimensional soil column model by Wise et al.[19] was adopted in this study. The length and height of the model are 10 m, the left and right boundary water heads are 10 m, and the upper and lower boundaries have no-flow boundaries. Then, at time 0, the right boundary water head is instantly reduced to 3 m, as shown in Fig. 8. For the value of L from large to small, the relationship between the change of groundwater level and L is analysed through numerical calculation. The unsaturated hydraulic parameters are calculated by Van Genuchen model, and the initial conditions are obtained by steady-state calculation. The relevant calculation parameters are the same as those of Wise et al.[19], as shown in Table 3.

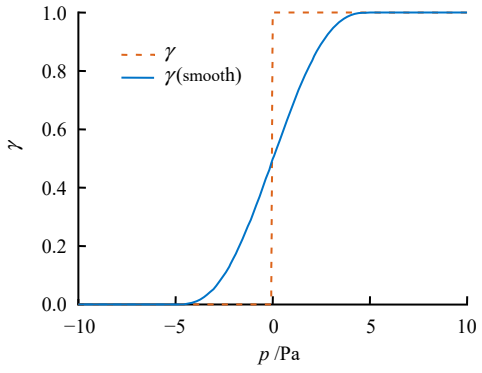

Fig. 7 Relationship between the function γ and p

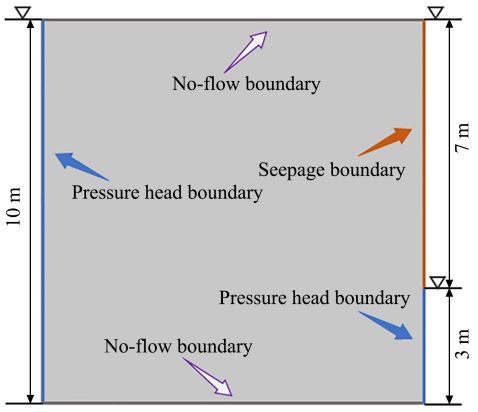

Fig. 8 Two-dimensional soil column model

Table 3 Relevant hydraulic parameters for calculation

Saturated volumetric water content θ_s	Residual volumetric water content θ_r	Saturated permeability coefficient K_s/(m • s^{-1})	Van Genuchen content		
			α	n	l
0.46	0.01	5.9×10^{-5}	2.0	2.8	0.5

In this study, the steady-state calculation of the model is first carried out to obtain the position of the groundwater level line when it finally reaches the steady-state. Different L values are adopted for finite element calculation, and the results are shown in Fig. 9. It can be seen from the figure that when the magnitude of L is greater than 10^{-3}, the position of the steady-state groundwater level line is on the high side; when L is equal to 10^{-3}, the position of the steady-state groundwater level line is the same as that calculated by Wise et al.[19]; and when the magnitude of L continues to decrease (L=10^{-4}), the position of the steady-state groundwater level line will not change. Therefore, when the magnitude of L is less than or equal to 10^{-3}, relatively accurate results can be obtained. For convenience, L can be unified as 10^{-3}.

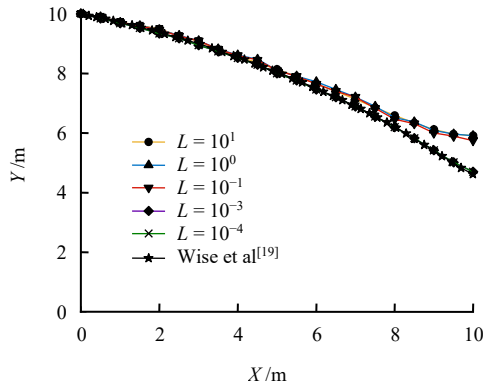

Fig. 9 Relationship between water table and L in steady state

In order to verify whether the above equation describing the seepage boundary and the value of L is reasonable, the transient calculation is carried out on the above model to obtain the positions of the groundwater line at different times, and the comparison is made with the calculation results of Wise et al.[19], as shown in Fig. 10. It can be seen from the figure that the results are in good consistency.

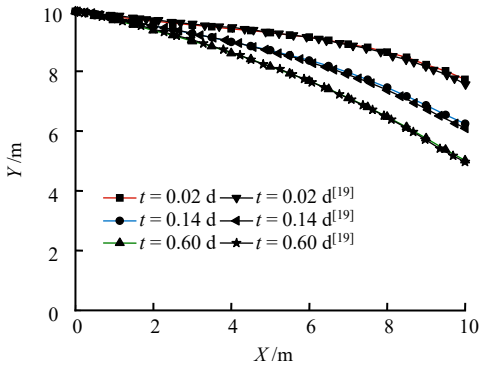

Fig. 10 Location of water table at different time

4 Slope case analysis

4.1 Geometric model and parameters

In this study, a homogeneous slope with a length of 34 m, a height of 20 m and a dip angle of 30° is taken as an example. In order to reduce the influence of the boundary on the calculation results, a slope geometric model with a length of 80 m and a height of 40 m is established, as shown in Fig. 11. The upper boundary of the model is the atmospheric boundary of the surface, the left boundary and the bottom boundary are the no-flow boundary, and the right boundary is composed of the upper seepage boundary and the pressure head boundary of the lower constant groundwater level. Since the surface pressure head changes dramatically during rainfall, in order to reduce the calculation workload and improve the accuracy of transient calculation, the mesh division of the lower layer of the model is relatively sparse, while the mesh division of the surface soil is very dense, which makes it more sensitive in the iterative calculation process.

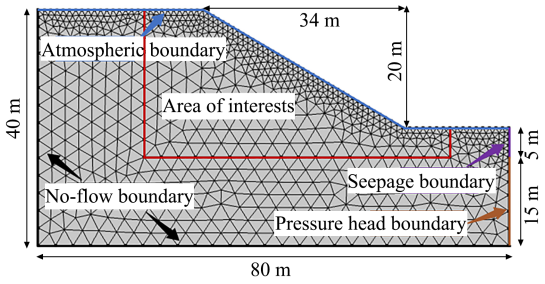

Fig. 11 Geometry of slope model

The part in the red frame in the geometric model of

the slope is the main study area for this numerical calculation, and its initial groundwater level and seepage process during rainfall are shown in Fig. 12. In the process of rainfall, when the wet front at the lower part of the slope reaches the initial groundwater level at first, the groundwater level will rise continuously, and the seepage flow on the right side will increase continuously. When the local groundwater level rises to the surface, surface seepage will be formed.

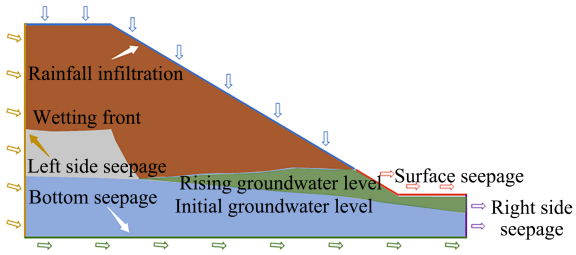

Fig. 12 Schematic diagram of seepage process in the area of interests

In this study, using COMSOL-multiphysics software, the governing equations of the above infiltration boundary conditions and seepage boundary conditions are respectively used to analyse the seepage law on the slope surface and inside the slope body under rainfall conditions through finite element calculation. The slope soil is seriously weathered silty soil with a porosity of 0.415. The Brooks-Corey model is used for unsaturated hydraulic parameters, and the relevant calculation parameters are shown in Table 4. The initial groundwater condition of the slope is obtained by steady-state seepage analysis with rainfall intensity of 0.24 mm /d[20]. The rainfall intensities of 4 mm /h and 40 mm /h are used to represent the situation that the rainfall intensity is less than the saturated permeability coefficient and the rainfall intensity is greater than the saturated permeability coefficient, respectively. Two typical rainfall conditions (long and weak, short and strong) are simulated and calculated, in which the rainfall duration of 4 mm /h is 200 h, and that of 40 mm /h is 20 h. The total rainfall of the two conditions is the same.

Table 4 Relevant hydraulic parameters for calculation

Saturated volumetric water content θ_s	Residual volumetric water content θ_r	Saturated permeability coefficient K_s /(m • s^{-1})	Brooks-Corey constant			Rainfall intensity /(mm • h^{-1})	
			α	n	l	R_1	R_2
0.415	0.041	7.19×10^{-6}	6.5	0.322	1	4	40

4.2 Volumetric moisture content

The distribution of volumetric water content of the soil in the studied area at different moments is shown in Fig. 13. As can be seen from the figure, when the rainfall is 4 mm /h, the infiltration of rainwater makes the volume moisture content of surface soil increase from 0.29 to 0.35 at the beginning, and the wetting front gradually develops downward. When the rainfall is 25 h, the wetting front at the foot of the slope seeps down to the initial groundwater level, making the groundwater level rise gradually. After 75 h of rainfall, the groundwater level at the foot of the slope rises to the surface. After 200 h of rainfall, the soil near the foot of the slope has reached saturation, and the soil under the top of the slope has not reached the initial groundwater level due to the long infiltration distance. When the rainfall intensity is 40 mm /h, the moisture content of the surface soil rapidly increases to 0.415 in a very short time, that is, it reaches saturation. After 4 h of rainfall, the wetting front at the foot of the slope reaches the initial groundwater level. After 9 h of rainfall, the soil near the foot of the slope has reached saturation. After 20 h of rainfall, the wetting front develops further downward, and the saturated area of soil near the foot of slope increases. Under the two rainfall intensities, the wetting front develops parallel to the surface and propagates downward. In general, the wetting front first reaches the groundwater level at the foot of the slope and then expands the saturated area continuously. The total rainfall is the same, and the infiltration depth of the former is greater than that of the latter.

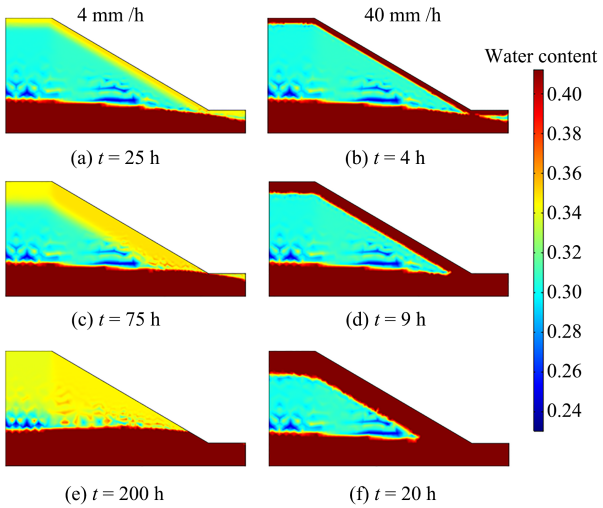

Fig. 13 Distribution of volume water content at different moments

4.3 Infiltration rate and pore water pressure

The actual infiltration rate and boundary pressure of surface soil in the studied area are shown in Figs. 14 and 15. As can be seen from the figure, when the rainfall intensity is 4 mm /h, the infiltration rate of the slope top is 1.10×10^{-6} m /s, equal to the rainfall intensity, and the

infiltration rate of the slope surface is 1.273×10^{-6} m /s, 1.15 times that of the slope top. As the flow velocity direction specified in the equation is the outer normal direction of the boundary, the slope inclines to increase the area of rainwater received at the same horizontal distance, hence the actual infiltration rate calculated is greater than the slope top. When the rainfall intensity is small, the error can be ignored. After rainwater infiltration, the pore water pressure of the surface soil increases from −22.59 kPa to −2.716 kPa and remains stable. When the rainfall intensity is 40 mm /h, the slope top and slope surface soil saturates within 1 h, the actual infiltration rate begins to reduce, and decrease quickly in 1−3 h. After 3 h, the infiltration rate has a slow decrease and is gradually close to the saturated permeability coefficient. The boundary pressure increases from the initial boundary pressure of −22.59 kPa to 97.351 Pa. In the infiltration boundary condition equation, the setting of the hydrops depth is 0.01 m, and the estimate should be 100 Pa, which is consistent with the previous one.

4.4 Infiltration amount and seepage discharge

Assuming that the longitudinal thickness of the two-dimensional slope model is 1 m, the actual infiltration rate of rainfall infiltration boundary in the studied area can be obtained by the line integral, and the infiltration

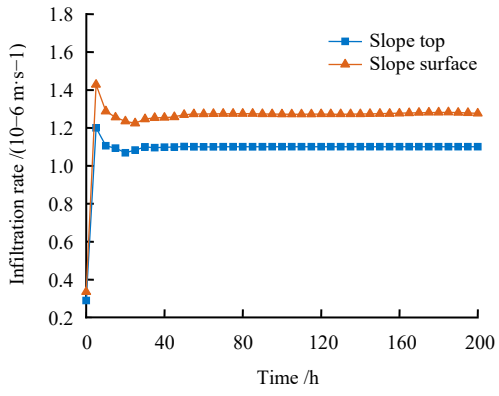

(a) 4 mm /h

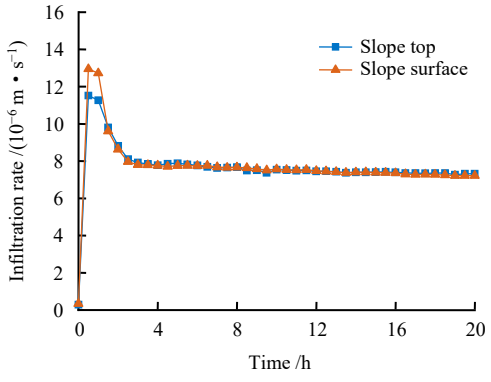

(b) 40 mm /h

Fig. 14 Evolution of infiltration rate with time under two rainfall intensities

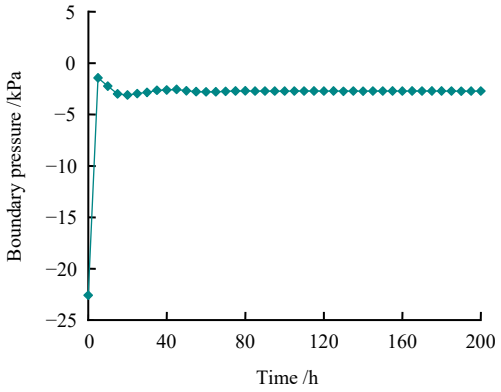

(a) 4 mm /h

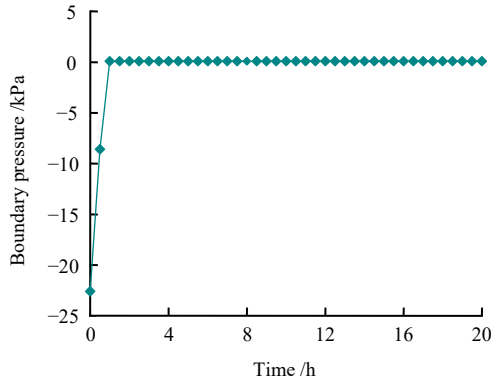

(b) 40 mm /h

Fig. 15 Evolution of boundary pressure with time under two rainfall intensities

amount of infiltration boundary at different times can be obtained, as shown in Fig. 16. As can be seen from the figure, when the rainfall intensity is 4 mm /h, the initial infiltration amount is equal to the rainfall, and all the rainwater penetrates into the soil. When the rainfall is at 75 h, the infiltration amount begins to decrease gradually. At this time, the groundwater level at the foot of the slope rises to the surface, and with the increase of the saturated area, the water in the slope begins to seep out continuously. When the rainfall intensity is 40 mm /h, for 1 h rainfall the surface soil saturates rapidly, all rainwater infiltrates into the soil (because at the beginning of the fitting process, there is the error in the calculation results in this stage). Within 1−3 h of rainfall, the infiltration rate decreases rapidly, leading to a rapid decrease in infiltration amount. After 4 h rainfall, the infiltration amount slowly begins to reduce, the wetting front reaches the underground water level, and the saturated area at the foot of the slope gradually expands. The calculation shows that under the condition of two kinds of rainfall the slope rainfall is 41 m^3. The total infiltration amount of studied area of slope can be obtained by accumulating the infiltration amount under the two rainfall intensities. The total infiltration amount is 39.068 m^3 when the rainfall is 4 mm /h for 200 h; and rainfall of 26.908 m^3 corresponds to the

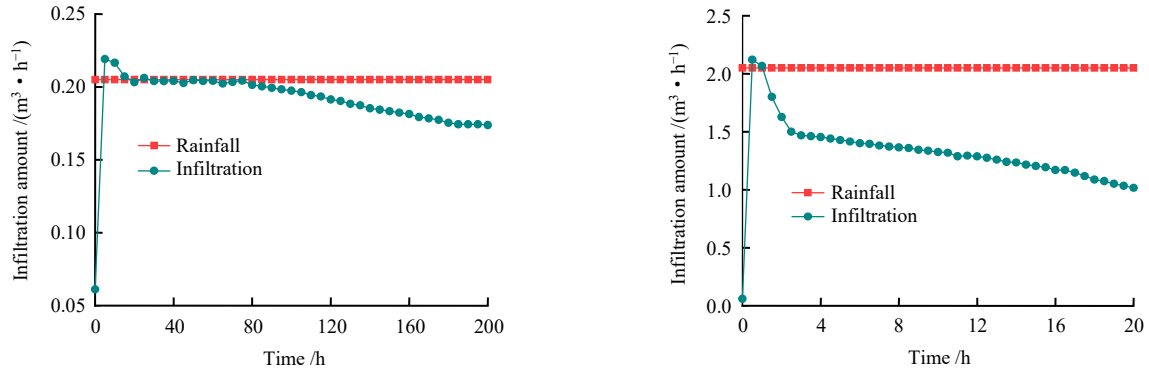

Fig. 16 Evolution of rainfall and infiltration amount with time

condition of 40 mm /h for 20 h. The former is much greater than the latter.

Figure 17 shows the variation rule of seepage flow at each boundary of the studied area with time. As can be seen from the figure, when the rainfall intensity is 4 mm /h, the infiltration depth increases with the increase of the rainfall duration, and the left infiltration amount gradually increases. When the rainfall is 25 h, the groundwater level at the foot of the slope rises, and the seepage flow on the right side begins to increase gradually. When the rainfall is 75 h, the groundwater level at the foot of the slope rises to the surface, forming surface seepage. With the increase of saturated area, the surface seepage flow gradually increases. At this time, the water in the slope flows more to the right, which also increases the bottom seepage. When the rainfall intensity is 40 mm /h, due to the larger infiltration rate, the seepage on the left side also increases faster. In the early stage of rainfall, the surface soil quickly reaches saturation and forms a transient saturation zone, so the seepage change on the right side is small. When the rainfall is 4 h, the wetting front at the foot of the slope reaches the groundwater level, which makes the seepage flow on the right side increase rapidly. At this time, the seepage flow on the bottom also increases, and the seepage flow on the surface begins to increase slowly. When the rainfall is 9 h, the soil at the foot of the slope reaches saturation, and the seepage flow on the right side and bottom begins to decrease, but with the increase of the saturated area. The surface seepage flow increases faster.

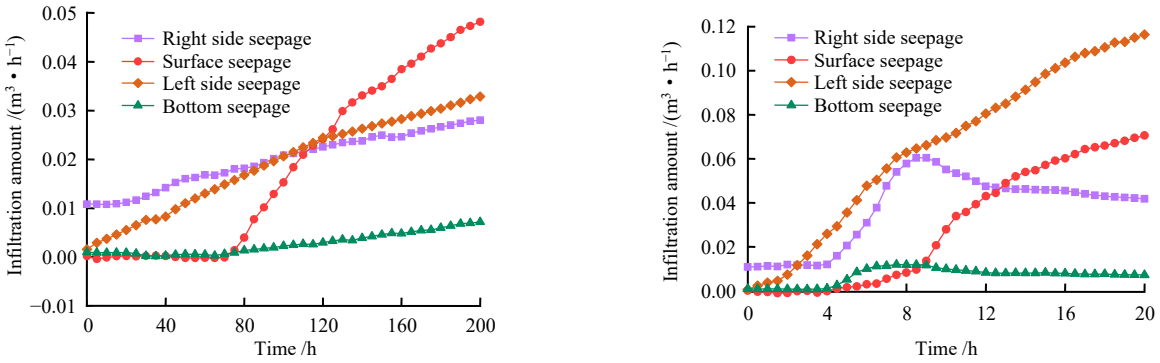

Fig. 17 Evolution of boundary seepage at the area of interests

5 Conclusion

Using COMSOL Multiphysics finite element code, based on the Richards equation of saturated−unsaturated seepage flow, the governing equations of the infiltration boundary conditions and seepage boundary conditions controlled by pore water pressure were respectively derived, and applied in the case of slope. The seepage laws of slope surface and slope body under rainfall condition were analysed, the conclusion is made as follows:

(1) According to the derived infiltration boundary conditions and seepage boundary conditions, based on the two-dimensional soil column model and the case model in the existing literature, the value of the boundary coupling length scale L was discussed respectively, and it was found that when the value of L was 0.001 m, the calculated results were in good agreement with the existing conclusions.

(2) Infiltration boundary conditions and seepage boundary condition were applied to a simple two-dimensional slope example. The different rainfall conditions (long and weak; short and strong), the change rule of volumetric moisture content in the slope were analysed. Results show that when the rainfall intensity was 4 mm /h, the volumetric water content of surface soil increased from the original 0.29 to 0.35, and gradually penetrate downward; when the rainfall intensity was 40 mm /h, the volumetric water content of the surface soil increased from 0.29 to 0.415 (reaching saturation) and gradually seeps downward. The infiltration depth of the former was greater than that of the latter with the same rainfall intensity.

(3) Analysis of the infiltration and seepage law of the slope showed that, when the rainfall intensity was 4 mm /h (less than the saturated permeability coefficient of the rock and soil mass of the slope), the actual infiltration rate was always equal to the rainfall intensity, the surface soil would not reach saturation and the pore water pressure increased to −2 176 Pa. When the rainfall intensity was 40 mm /h (greater than saturated permeability coefficient of the slope rock mass), the surface soil was saturated in a short time, the actual infiltration rate was equal to the rainfall intensity at first, and gradually decreased after the surface soil was saturated until it was close to the saturated permeability coefficient. The boundary pressure increased to 97.351 Pa (related to the setting of the hydrops depth).

(4) On the slope infiltration and seepage flow analysis, the total rainfall in the studied slope area under the two rainfall conditions was 41 m^3. For 4 mm /h rainfall intensity with a rainfall of 200 h, the total infiltration amount in the studied area was 39.068 m^3. For 4 mm /h of rainfall intensity with a rainfall of 200 h, the total infiltration amount in the studied area was 26.908 m^3. The former was much larger than the latter, and the seepage inside the slope were obviously different the surface seepage at the foot of the slope under the two rainfall conditions.

References

[1] NG Charles W W, CHEN Shou-yi, PANG Yu-wei. Parametric study of effects of rain infiltration on unsaturated slopes[J]. Rock and Soil Mechanics, 1999, 20(1): 1−14.

[2] LI Zhao-ping, ZHANG Mi. Effects of rain infiltration on transient safety of unsaturated soil slope[J]. China Civil Engineering Journal, 2001, 34(5): 57−61.

[3] ZHANG Pei-wen, LIU De-fu, HUANG Da-hai. Saturated-unsaturated unsteady seepage flow numerical simulation[J]. Rock and Soil Mechanics, 2003, 24(6): 927−930.

[4] RONG Guan, ZHANG Wei, ZHOU Chuang-bing. Numerical analysis of saturated-unsaturated seepage problem of rock slope under rainfall infiltration[J]. Rock and Soil Mechanics, 2005, 26(10): 24−29.

[5] JANG Zhong-ming, XIONG Xiao-hu, ZENG Ling. Unsaturated seepage analysis of slope under rainfall condition based on FLAC^{3D}[J]. Rock and Soil Mechanics, 2014, 35(3): 855−861.

[6] JANG Shui-hua, LIU Xian, HUANG Fa-ming, et al. Failure mechanism and reliability analysis of soil slopes under rainfall infiltration considering spatial variability of multiple soil parameters[J]. Chinese Journal of Geotechnical Engineering, 2020, 42(5): 900−907.

[7] WANG Hua-bin, LI Jian-mei, JIN Yi-xuan, et al. The numerical methods for two key problems in rainfall- induced slope failure[J]. Rock and Soil Mechanics, 2019, 40(2): 777−784.

[8] YE Zu-yang, JANG Qing-hui, LIU Yan-zhang. Numerical analysis of unsaturated seepage flow in discrete fracture networks of rock[J]. Rock and Soil Mechanics, 2017, 38(11): 3332−3339.

[9] REN Qing-wen, ZHANG Lin-fei, SHEN Lei. Analysis of deformation law of rock mass considering unsaturated seepage process[J]. Chinese Journal of Rock Mechanics and Engineering, 2018, 37(Suppl.2): 4101−4107.

[10] SHAO Jian-li, ZHOU Fei, XUE Yan-chao. Study on numerical simulation of pore-fracture double seepage in rock mass[J]. Journal of Coal Mine Safety, 2019, 50(9): 1−4.

[11] COMSOL A. COMSOL Multiphysics user's guide[M]. [S. l.]: [s. n.], 2013.

[12] LI Guang-xin. Advanced soil mechanics[M]. 2nd ed. Beijing: Tsinghua University Press, 2016: 50−65.

[13] GERKE H H, VAN GENUCHTEN M T. A dual-porosity model for simulating the preferential movement of water and solutes in structured porous media[J]. Water Resources Research, 1993, 29(2): 305−319.

[14] ZOU Li-zhi. Futher discussion on the concepts of water storage rate and water storage coefficient[J]. Hydrogeology & Engineering Geology, 1989(3): 50−52.

[15] VAN GENUCHTEN M T. A closed-form equation for predicting the hydraulic conductivity of unsaturated soils[J]. Soil Science Society of America Journal, 1980, 44(5): 892−898.

[16] BROOKS R H, COREY A T. Properties of porous media affecting fluid flow[J]. Journal of the Irrigation and Drainage Division, 1966, 92(2): 61−90.

[17] MEIN R G, LARSON C L. Modeling infiltration during a steady rain[J]. Water Resources Research, 1973, 9(2): 384−394.

[18] MAY CHUI T F, FREYBERG D L. Implementing hydrologic boundary conditions in a multiphysics model[J]. Journal of Hydrologic Engineering, 2009, 14(12): 1374−1377.

[19] WISE W R, CLEMENT T P, MOLZ F J. Variably saturated modeling of transient drainage: Sensitivity to soil properties[J]. Journal of Hydrology, 1994, 161(1-4): 91−108.

[20] XIE Ding-yi. Soil mechanics for unsaturated soils[M]. Beijing: Higher Education Press, 2015: 309−312.